ELSEVIER

Chemical Geology 236 (2007) 291–302

CHEMICAL GEOLOGY
INCLUDING
ISOTOPE GEOSCIENCE

www.elsevier.com/locate/chemgeo

Nd–Hf–Sr–Pb isotopes and trace element geochemistry of Proterozoic lamproites from southern India: Subducted komatiite in the source

Ramananda Chakrabarti [a], Asish R. Basu [a,*], Dalim K. Paul [b]

[a] *Department of Earth and Environmental Sciences, University of Rochester, Rochester, NY-14627, USA*
[b] *Department of Geology, Presidency College, Calcutta, 700073, India*

Received 8 February 2006; received in revised form 17 August 2006; accepted 15 October 2006

Editor: S.L. Goldstein

Abstract

The probable sources of some of the famous Indian diamonds are the 1.2 Ga old Krishna lamproites of Southern India, a rare Proterozoic occurrence of lamproites which are usually Cretaceous or younger in age. In this study we report Nd, Sr, Pb and Hf isotopes and multiple trace element concentrations of the Krishna lamproites. The goals are to evaluate mantle-processes and the petrogenesis of these ultrapotassic rocks of extreme chemical composition in light of these geochemical data, including their major element compositions.

The Krishna lamproites show nearly uniform, parallel rare earth element (REE) distribution patterns with high concentrations and extreme light-REE enrichment ($La/Yb_{(N)}$=41–88), high average concentrations of Ba (~1200 ppm), Sr (~1200 ppm), Zr (~930 ppm), La (~230 ppm), high U/Pb and Th/U ratios with notable absence of any Eu-anomaly. These rocks are typically porphyritic without any evidence of crystal accumulation, and have moderately high Mg-numbers (59–73) along with high Ni (average ~301 ppm, highest 819 ppm) and Cr (average ~183 ppm, highest 515 ppm) concentrations that show a positive correlation with MgO (wt.%), implying a role of olivine in the melt source. The low SiO_2 content (lowest 37.8%, average 49%) and high Nb (average 147 ppm), Zr, Sr, as well as Ni and Cr in these rocks indicate lack of upper continental crustal contribution in the genesis of these rocks. The initial Pb-isotopic composition of these lamproites is unusual in that in a $^{207}Pb/^{204}Pb$ vs. $^{206}Pb/^{204}Pb$ plot, these rocks plot to the left of the 1.2 Ga geochron (age of emplacement), unlike most mantle-derived rocks. This Pb-isotopic signature and the superchondritic Nb/Ta ratios (average 23.6) of these rocks rule out their derivation from a metasomatized sub-continental lithospheric mantle. The high $^{207}Pb/^{204}Pb$ at low $^{206}Pb/^{204}Pb$ indicates an Archean component in the source of these rocks. We argue that this Archean crustal component, which produced the low-SiO_2 lamproites along with the high Ni and Cr must have been ultrabasic, and we propose a model in which these lamproites formed by partial melting of metasomatized, subducted Archean komatiite in a peridotite mantle-source assemblage. In addition, these rocks display initial Hf isotopic compositions similar to Al-depleted komatiites, and high Nb/U, Nb/Th, and TiO_2 as well as low Al_2O_3/TiO_2 ratios (1.1–4.2) and average CaO/Al_2O_3 of ~1.6 that are also similar to Archean komatiites. This is also supported by the initial Pb isotopic composition of the Krishna lamproites, requiring evolution in a variably high U/Pb, Th/Pb reservoir early in earth history, possibly resulting from preferential segregation of Pb relative to U and Th in the sulfides of the komatiite.

* Corresponding author. Fax: +1 585 244 5689.
E-mail address: abasu@earth.rochester.edu (A.R. Basu).

0009-2541/$ - see front matter
doi:10.1016/j.chemgeo.2006.10.006

The Al-depleted subducted komatiitic component was enriched by carbonate metasomatism in the peridotitic mantle. This metasomatism was responsible for the observed Nd–Hf isotope characteristics, specifically variable $\varepsilon_{Nd(T)}$ at relatively constant $\varepsilon_{Hf(T)}$ in the lamproites. This Nd–Hf-isotopic characteristic seems to be common in global lamproites of all ages. Our proposed model for the genesis of the Krishna lamproites involving a subducted komatiitic source may also be applicable for other global lamproites from cratonic settings, as older komatiite-bearing subducted crustal components were possibly ubiquitous in the architecture of ancient cratonic mantle.

Keywords: Proterozoic lamproites; Nd–Sr–Hf–Pb isotopes; Major and trace elements; Petrogenesis; Subducted Al-depleted komatiite

1. Introduction

Lamproites and kimberlites show one of the most extreme chemical compositions of the magmas reaching the Earth's surface. Their ultrapotassic composition and wide ranging modal mineralogy (Mitchell and Bergman, 1991) are thought to be derived from a geochemically anomalous mantle (Basu and Tatsumoto, 1979; Kramers et al., 1981). Lamproites are found in several tectonic settings, most of them seem to be post-tectonic and occur at cratonic margins, while others occur within cratons and in accreted mobile belts. While most global occurrences of these rocks are Cretaceous and younger in age, Proterozoic lamproites are rare and not well studied. There are however, reported occurrences of Proterozoic kimberlites, lamproites and related alkalic rocks from worldwide localities including Canada, Greenland, South Africa, West Africa and Australia, all with relatively close emplacement ages at around 1100–1200 Ma. Skinner et al. (1985) consider this period between 1100–1200 Ma as an important world-wide "mantle event" related to lamproite and kimberlite emplacement. Several Proterozoic lamproites have recently been reported from the Archean eastern Dharwar craton and the adjoining Proterozoic Cuddapah sedimentary basin of southern India (Rao et al., 2004). The present study focuses on the Proterozoic Krishna lamproites (Fig. 1), which are one of the oldest lamproites in the world with an Rb–Sr age of 1224±14 Ma (Kumar et al., 2001) and are thought to be the sources of the famous Indian diamonds, Kohinoor, Hope, Regent, Nizam and several others.

Global lamproites are characterized by high K_2O, MgO and NiO contents and low CaO, Al_2O_3 and Na_2O (Foley et al., 1987; Mitchell and Bergman, 1991) with distinctively low Nb, Ta, Sr and high Ba contents, relative to the primitive mantle. They display variable but radiogenic Sr-isotopic composition and strongly negative $\varepsilon_{Nd(0)}$ values; the Pb-isotopic compositions are also extremely variable and different for each lamproite province, implying that the μ values ($^{238}U/^{204}Pb$) of their source regions were very heterogeneous. Lamproites are geochemically similar to Group II kimberlites (orangeites) in many respects, especially in their high rare earth element (REE) contents, light-REE enrichment and less-radiogenic Nd-isotopic compositions, and are in contrast with Group I kimberlites that have more radiogenic Nd-isotopic compositions. However, there are significant mineralogical differences between lamproites and Group II kimberlites and direct comparisons of these two rock types are not useful (Mitchell and Bergman, 1991).

The present multiple trace element and Nd, Sr, Hf, and Pb-isotopic study of one of the most ancient lamproites from the southern Indian craton was undertaken to evaluate their petrogenesis and also for understanding possible deep subcontinental mantle processes involved in the generation of the partial melts of lamproites of extreme chemical signatures during the mid-Proterozoic. Because of their ancient age and mode of occurrence in the Indian craton with well-known tectonic provenances, it was expected that such a study might provide new perspectives in lamproite genesis. Based on our geochemical data of the lamproites, we propose a model in which lamproites are generated by partial melting of a mantle peridotite assemblage containing a subducted komatiite-bearing component.

2. Geologic setting and samples for this study

The Krishna lamproites occur in the northeastern part of the Proterozoic Cuddapah sedimentary basin of southern India, which is sandwiched between the Archean Dharwar cratonic rocks to the west and Mesoproterozoic granulites of the Eastern Ghat mobile belt to the east (Fig. 1). These ultrabasic rocks occur mostly as dikes and rarely as plugs and are hosted by early Proterozoic granites of the Peninsular Gneissic Complex of the Dharwar craton. The Krishna lamproite field covers an area of 160 km^2, comprising more than 30 exposed lamproite bodies. Our study is confined to these ultrabasic rocks occurring around Ramnapeta (KLR), Jayantipuram (KLJ), Vedadri (KLV), Pochampalle

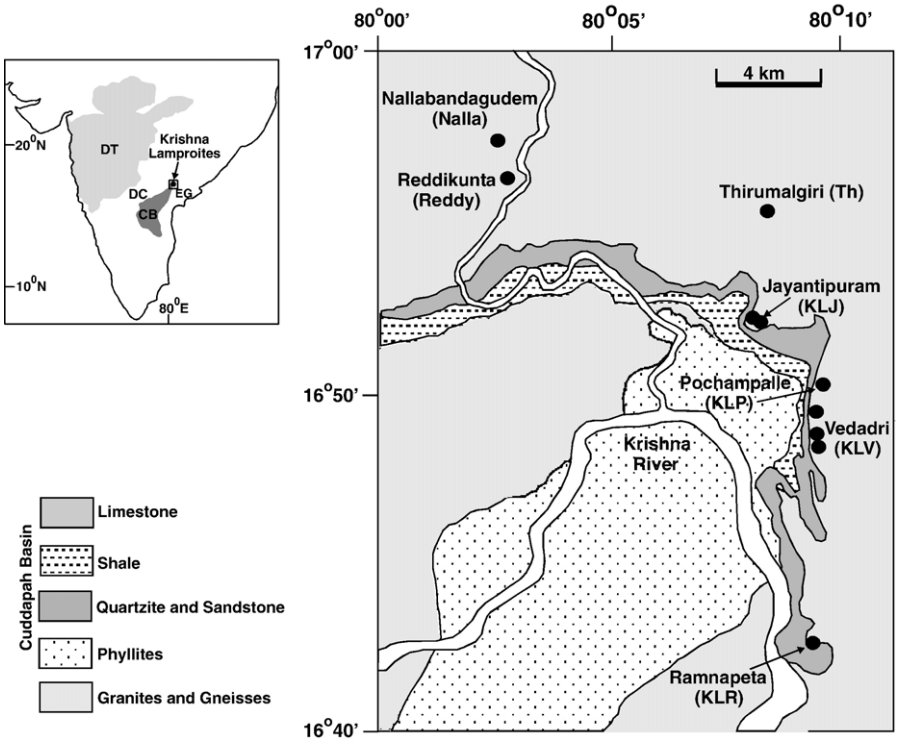

Fig. 1. Geological map of the Krishna lamproite field showing the locations of the lamproite samples analyzed in the present study. The Krishna lamproites are hosted by the early Proterozoic Penninsular gneissic complex and occur in the northeastern part of the Proterozoic Cuddapah sedimentary basin. Also shown (inset) is the map of Peninsular India showing the Krishna lamproite field (filled circle), Deccan Traps (DT), Archean Dharwar craton (DC), Proterozoic Cuddapah Basin (CB) and the Proterozoic Eastern Ghats Mobile Belt (EG).

(KLP), Thirumalgiri (Th), Nallabandagudem (Nalla) and Reddikunta (Reddy) (Fig. 1). Detailed petrographic and field descriptions of the samples are being reported elsewhere (Paul et al., in preparation) and only a brief summary is given here. Common minerals include olivine (often serpentinized), phlogopite, alkali feldspar, diopside, apatite, chlorite, sphene, biotite, perovskite, opaques and carbonates. The Krishna lamproites are clearly porphyritic with phenocrysts of phlogopite and olivine in a fine-grained groundmass. The phenocrysts are uniformly distributed without any evidence of crystal settling. These lamproites are often found in association with diabase dikes and contain xenocrysts or megacrysts of pyrope-rich garnet and diopside. However, no mantle-derived peridotite or eclogite xenoliths have yet been reported from them, although these rocks are believed to be the sources of the most well-known Indian diamonds. Based on detailed petrography of the Krishna lamproites, these rocks can be classified as diopside lamproites, phlogopite lamproites and olivine lamproites (Rao et al., 2004; Paul et al., in preparation). A Rb–Sr age of 1224±14 Ma (Kumar et al., 2001) has been determined for the emplacement of these lamproites.

3. Analytical methods

Ten lamproite samples from the Krishna lamproite field were analyzed for their trace element concentrations and high-precision Sr-, Nd-, Hf-, and Pb-isotopic

Table 1
Summary of major element concentration data for the Krishna lamproites ($n=10$) from Paul et al. (in preparation)

	Concentration ranges (wt.%)	Average concentration (wt.%)
SiO_2	37.8–61.6	49.0
TiO_2	2.6–5.2	4.0
Al_2O_3	4.4–10.7	6.7
Fe_2O_3	6.7–11.7	9.5
MnO	0.09–0.2	0.13
MgO	5.4–15.6	9.9
CaO	6.7–13.3	9.8
Na_2O	0.13–1.1	0.8
K_2O	1.1–6.1	2.4
P_2O_5	0.9–3.0	1.6
Mg#	59–73	66
CaO/Al_2O_3	0.6–2.3	1.6
Al_2O_3/TiO_2	1.1–4.2	1.8

ratio measurements. Samples were powdered using a Spex® alumina ball mill. Trace element concentrations were measured using an Inductively Coupled Plasma Mass Spectrometer (Thermo elemental X-7 series) at the University of Rochester. 25-mg powdered samples were digested using HF–HNO_3 acid mixtures and diluted to 100 ml of 2% HNO_3 solution with ~10 ppb internal standard of In, Cs, Re, and Bi. BCR-2 and BIR-2 (basalts-USGS) were used as known external standards while AGV-2 (andesite-USGS) and BHVO-2 (basalt-USGS) rock standards were run as unknowns to estimate the error. Analytical uncertainties are usually less than 5% for most of the trace elements and commonly less than 2% for the REEs.

Nd-, Sr-, and Pb-isotopic ratios were measured with a multi-collector Thermal Ionization Mass Spectrometer (TIMS, VG Sector) for which 100–200 mg powdered rock samples were dissolved in HF–HNO_3 and HCl acids. Nd and Sr-isotopes were measured using the procedures established for our laboratory at the University of Rochester (Basu et al., 1990). Measured $^{87}Sr/^{86}Sr$ ratios were normalized to $^{86}Sr/^{88}Sr=0.1194$. Uncertainties for the measured $^{87}Sr/^{86}Sr$ were less than 4 in the 5th decimal place. The NBS-987 Sr standard analyzed during the course of this study yielded $^{87}Sr/^{86}Sr=0.710245\pm0.000023$ (2σ) ($n=5$). Measured $^{143}Nd/^{144}Nd$ ratios were normalized to $^{146}Nd/^{144}Nd=0.7219$ (O'Nions et al., 1977). Uncertainties for the measured $^{143}Nd/^{144}Nd$ ratios were less than 3 in the 5th decimal place. La Jolla Nd-standard analyzed during the course of this study yielded $^{143}Nd/^{144}Nd=0.511852\pm24$ (2σ) ($n=4$) where the errors correspond to the last two digits. Initial ε_{Nd} values were calculated using present day Bulk Earth $^{143}Nd/^{144}Nd$ of 0.512638 and $^{147}Sm/^{144}Nd$

Table 2
Trace element concentrations and some elemental ratios of the Krishna lamproites

Samples	Th 3/1	KLR-1	KLV-2	KLJ-2	Reddy	KLP-1	KLV-1	Nalla	KLJ-1	KLV-3
Ti	2896.0	1880.0	2761.0	3413.0	2975.0	1425.0	2114.0	3002.0	2373.0	1658.0
Cr	21.3	277.8	217.7	140.3	111.5	218.7	107.8	85.5	134.8	515.0
Ni	65.1	385.2	351.8	254.2	202.8	241.5	298.3	216.3	175.7	819.1
Rb	49.0	46.8	5.9	30.7	111.4	398.1	50.5	56.8	5.7	3.5
Sr	1486.0	892.4	1905.0	488.7	1826.0	829.1	1595.0	1840.0	935.4	455.1
Y	61.1	19.5	48.9	58.6	44.6	43.4	43.4	41.8	55.5	35.4
Zr	843.6	401.0	1323.0	795.3	990.0	1458.0	847.5	1067.0	1237.0	351.5
Nb	154.4	133.5	151.4	249.1	149.5	112.8	80.7	183.9	138.3	119.7
Ba	543.6	1874.0	999.2	419.5	671.2	4761.0	541.0	751.7	141.1	92.6
La	200.4	158.2	229.1	222.9	257.1	383.4	280.9	226.9	193.8	122.1
Ce	399.8	308.1	454.9	449.4	504.1	811.2	581.2	458.0	378.1	289.7
Pr	39.0	29.2	44.8	43.2	49.5	78.3	55.5	43.6	35.4	30.6
Nd	139.1	99.8	153.3	146.5	176.0	255.7	185.4	152.8	123.2	110.8
Sm	22.6	14.1	23.4	21.9	27.4	33.3	23.9	22.9	18.5	17.7
Eu	5.7	3.7	6.2	5.8	8.2	6.7	5.2	5.8	4.6	4.3
Gd	16.8	9.4	16.6	16.1	19.3	20.0	15.3	16.2	14.2	12.7
Tb	2.1	1.1	2.1	2.1	2.3	2.0	1.8	1.9	1.9	1.5
Dy	10.0	4.7	10.3	10.8	10.4	8.8	8.6	8.9	9.6	7.2
Ho	1.8	0.8	1.8	2.0	1.7	1.5	1.5	1.6	1.8	1.3
Er	4.1	1.7	4.0	4.3	3.6	3.4	3.4	3.4	4.2	2.8
Tm	0.51	0.21	0.51	0.49	0.43	0.46	0.41	0.42	0.51	0.35
Yb	2.9	1.3	3.0	2.6	2.6	3.0	2.4	2.5	2.8	2.0
Lu	0.32	0.16	0.32	0.28	0.27	0.33	0.26	0.25	0.28	0.23
Hf	19.6	9.4	30.1	18.8	22.5	30.8	18.1	24.5	28.5	7.5
Ta	6.1	6.2	5.8	8.4	6.4	5.1	5.1	7.7	5.3	5.6
Pb	8.5	27.1	12.6	6.9	25.3	34.3	18.9	14.9	7.1	43.0
Th	15.0	11.7	24.0	14.8	20.2	112.0	16.0	13.6	16.2	12.2
U	2.0	1.1	3.7	2.7	2.9	17.6	3.5	2.7	2.8	1.2
$La/Yb_{(N)}$	46.8	80.0	51.0	57.4	67.5	87.7	79.9	61.7	46.4	41.5
$Dy/Yb_{(N)}$	2.24	2.3	2.2	2.7	2.6	1.9	2.4	2.3	2.2	2.3
Th/U	7.5	10.7	6.4	5.5	7.1	6.4	4.6	5.1	5.7	9.9
Nb/U	244.1	144.0	329.8	58.5	284.5	163.0	312.1	240.1	177.0	81.6
Nb/Th	75.7	94.6	63.3	26.0	81.1	26.9	88.4	75.2	32.8	60.8
Nb/Ta	25.4	21.5	26.2	29.8	23.3	22.2	15.8	24.0	26.2	21.5
Zr/Hf	43.0	42.5	44.0	42.3	44.0	47.4	47.0	43.6	43.4	47.0

The concentrations are shown in μg/g (ppm) and were determined by ICPMS.

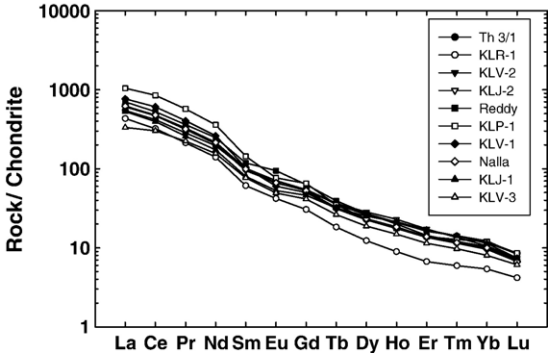

Fig. 2. Chondrite normalized Rare Earth Element (REE) patterns of the Krishna lamproites. The REE plots show a nearly uniform, parallel distribution pattern. The rocks show very high concentrations of the REEs, extreme light-REE enrichment, slightly flattened heavy-REE patterns and are characterized by the absence of Eu-anomaly.

of 0.1966 (Jacobsen and Wasserburg, 1980). Pb isotopes were measured using the silica-gel technique (Sharma et al., 1992) in our laboratory. Filament temperature during Pb-isotope ratio measurements was monitored continuously and raw ratios were calculated as weighted averages of the ratios measured at 1150 °C, 1200 °C and 1250 °C, respectively. The reported Pb-isotopic data were corrected for mass fractionation of 0.12±0.03% per amu based on replicate analyses of the NBS-981 Equal Atom Pb standard measured in the same fashion. Estimated errors are less than 0.05% per mass unit. Our laboratory procedural blanks were less than 400 pg for Sr and less than 200 pg for both Nd and Pb. No blank correction was necessary for the isotope ratios measured.

Hf-isotopic ratios were measured at the University of Rochester using a multi-collector Inductively Coupled Plasma Mass Spectrometer (MC-ICPMS, P-54) following the procedures of Blichert-Toft et al. (1997). For Hf separation, whole rock powders were dissolved using concentrated HF–HNO_3 acid mixtures. The residue was treated with concentrated HNO_3 and picked up in 1.5 M HCl and passed through a cation exchange resin column where Hf was separated from the REE. This eluent was then passed through an anion exchange resin to collect Hf, Ti, Zr and Cr. A final cation exchange resin separated Hf and Zr from Ti and Cr. The Hf–Zr separates were run on the MC-ICP-MS. Measured $^{176}Hf/^{177}Hf$ ratios were normalized to $^{179}Hf/^{177}Hf=0.7325$. Uncertainties for the measured $^{176}Hf/^{177}Hf$ were less than 2 in the 5th decimal place. JMC 475 Hf standard analyzed during the course of this study yielded $^{176}Hf/^{177}Hf=0.282157\pm10$ (2σ) ($n=4$) where the two standard errors correspond to the 5th decimal place. Initial ε_{Hf} values were calculated using the present day CHUR values of 0.282772 for $^{176}Hf/^{177}Hf$ and 0.0332 for $^{176}Lu/^{177}Hf$ (Blichert-Toft and Albarede, 1997) and the ^{176}Lu decay constant of Bizzarro et al. (2003). Our laboratory procedural blanks were less than 25 pg for Hf and no blank correction was necessary for the isotope ratios measured.

4. Analytical results

4.1. Trace element geochemistry of the Krishna Lamproites

Major element chemical composition of the Krishna lamproites are given in Paul et al. (in preparation) and only a relevant summary is presented here (Table 1). The Krishna lamproites have variable MgO (5.4–15.6 wt.%) and SiO_2 contents ranging from as low as 37.8 wt.% to an average of ~49 wt.%. They have average molar K_2O/Na_2O ratios >3, molar K_2O/Al_2O_3 ratios >0.8, (Paul et al., in preparation). Low K_2O/Na_2O and K_2O/Al_2O_3 in some samples are due to post-emplacement surficial chemical weathering, especially leaching of potassium in this monsoon-affected region. These rocks show low Al_2O_3/TiO_2 ratios (1.1–4.2) and average CaO/Al_2O_3 of ~1.6.

Our analytical results show that these rocks have high concentrations of Ba (average ~1200 ppm), Sr (average ~1200 ppm), Zr (average ~900 ppm) and La (average ~230 ppm) (Table 2), conforming to the chemical characteristics of lamproites *sensu stricto* (Mitchell and Bergman, 1991; Woolley et al., 1996). Chondrite-normalized rare earth element (REE) patterns of these rocks are shown in Fig. 2. As seen in Table 2

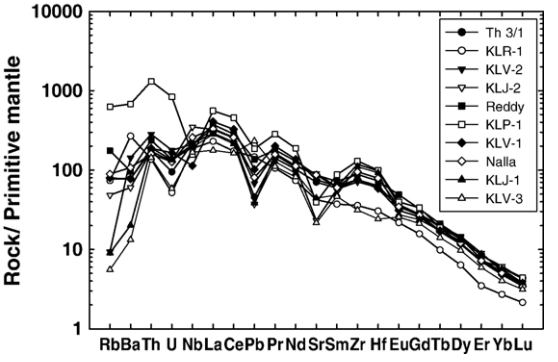

Fig. 3. Primitive mantle normalized multiple trace element patterns of the Krishna lamproites. Rb and Ba show a wide range in concentrations but have lower primitive mantle-normalized values with respect to Th. KLP-1 has higher concentrations of Rb, Ba, Th, and U compared to the other samples. Some samples show negative Sr and Pb anomalies while some others show positive Zr and Hf anomalies. No significant negative Nb anomaly is seen. These samples have high Nb/U ratios.

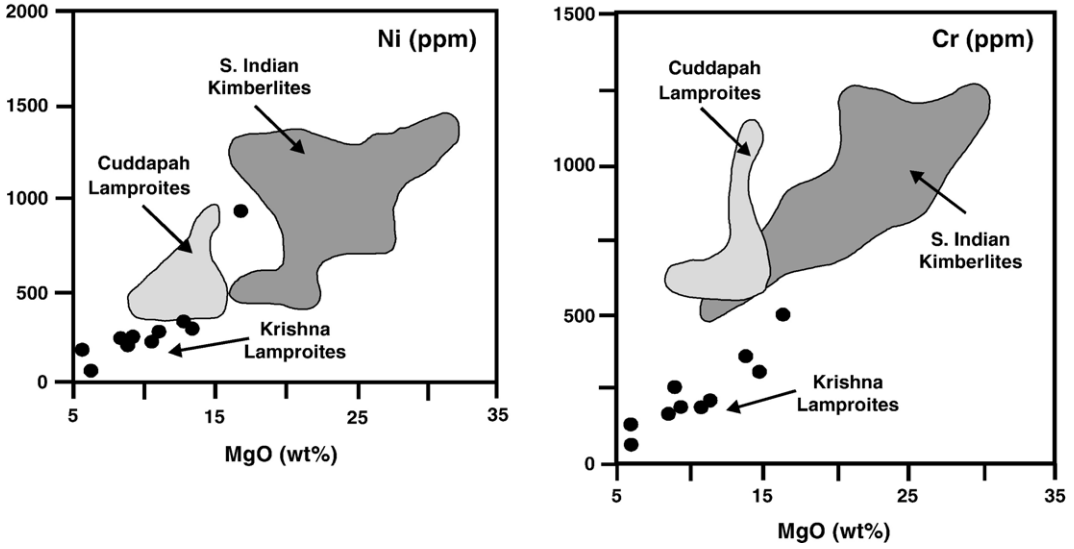

Fig. 4. The Krishna lamproites show high Ni and Cr concentrations and a positive correlation with MgO wt.% (Paul et al., in preparation), indicating contribution of olivine in the source of the melts as these rocks do not show any evidence of olivine accumulation. Also shown are the fields of kimberlites and lamproites from Southern India (Rao et al., 2004).

and Fig. 2, the Krishna lamproites have high concentrations of the REEs with extreme light-REE (LREE) enrichment ($La/Yb_{(N)}$=41.5–87.7) (Table 2), similar to most global lamproites and Group II kimberlites (Cullers et al., 1985; Foley et al., 1987; Mitchell and Bergman, 1991). They show a comparatively less steep heavy-REE (HREE) pattern ($Dy/Yb_{(N)}$=1.9–2.7) (Table 2) and are characterized by the notable absence of Eu-anomaly (Fig. 2).

Whole rock multiple trace element data of the lamproites are shown in Fig. 3 in a spider diagram normalized to the primitive mantle values of the elements (Sun and McDonough, 1989) and plotted with progressively less incompatible elements to the right. Among the most incompatible elements, Rb and Ba show a wide range in concentrations (Fig. 3). All rocks show high Th/Ba and Th/Rb ratios. The lamproites have variable but high U/Pb (2.1–37.2, average μ=17.2) and Th/U (4.6–10.7, average ~ 7) ratios. Th, U, Nb concentrations are similar for all the samples except for KLP-1. The lamproites show negative Sr and Pb anomalies in the primitive mantle normalized plot of Fig. 3. Except for KLV-3 and KLR-1, the lamproites also show positive Zr and Hf anomalies. However, no significant negative Nb anomaly is seen in any of the samples analyzed in this study. The rocks display high Ni (average ~ 301 ppm, highest 819 ppm) and Cr (average ~ 183 ppm, highest 515 ppm) contents (Table 2). These elemental concentrations are, however, lower compared to other southern Indian kimberlites and lamproites (Fig. 4). Ni and Cr also show a positive correlation with MgO (wt.%) in the Krishna lamproites as well as in the southern Indian kimberlites and lamproites (Fig. 4). These rocks display a positive correlation in a plot of Nb/Th vs. Nb/U (Fig. 5). High Nb/U (average 59) and Nb/Th (average 9) ratios are noteworthy, similar to Archean komatiites (Sylvester et al., 1997; Puchtel et al., 1998; Polat and Kerrich, 2000; Xie et al., 2000; Campbell, 2002) (Fig. 5) although the Krishna lamproites show a wider range in Nb/U ratios compared to the komatiites.

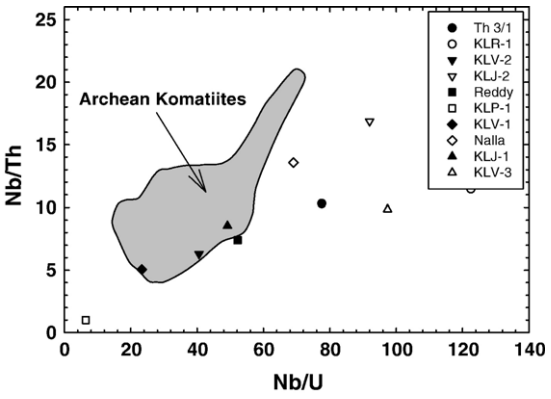

Fig. 5. Comparison of Nb/U and Nb/Th in the Krishna lamproites with those of Archean komatiites (Campbell, 2002). The Krishna lamproites (symbols same as Fig. 2) display a positive correlation between Nb/U and Nb/Th with high average Nb/U (~ 59) and Nb/Th (~ 9) similar to Archean komatiites. The wide range of Nb/U ratios of the lamproites is possibly due to post-emplacement mobilization of U.

4.2. Sr–Nd–Hf–Pb isotope geochemistry of Krishna lamproites

Nd, Sr, Pb and Hf-isotopic compositions of the Krishna lamproites are shown in Table 3. The initial isotopic ratios of these elements are calculated based on the ~1224 Ma Rb–Sr age of emplacement for these lamproites (Kumar et al., 2001). The initial Sr-isotopic ratios of the lamproites vary from 0.70096–0.70665 as shown in Fig. 6 along with their initial Nd isotopic composition. Sample KLP-1 has unusually high present-day Sr-isotopic composition and also the lowest initial Sr-isotopic ratio of 0.70096 (Table 3 and Fig. 6). Like other global lamproites, most of the Krishna lamproites have negative initial ε_{Nd} and radiogenic Sr-isotopic composition and lie in the time-integrated Rb/Sr and Nd/Sm enriched quadrant of the Nd–Sr isotopic diagram (Fig. 6). While their Nd-isotopic composition is similar to Group II kimberlites in Fig. 6, the Krishna lamproites show variable initial Sr-isotopic composition.

Initial Nd and Hf isotopic compositions of the Krishna lamproites are shown in Fig. 7 and are found to be similar to the global Group II kimberlites (Nowell et al., 2004). Their initial Hf isotopic composition overlaps with those of Al-depleted Barberton komatiites at 1224 Ma (Blichert-Toft and Arndt, 1999). $\varepsilon_{Nd(0)}$ values range from −30.4 to −22.6 while $\varepsilon_{Hf(0)}$ values range from −41.1 to −30.1 (Table 3). Compared to other global lamproites that are considerably younger in age (Nowell et al., 2004), the Krishna lamproites have more radiogenic initial Nd and Hf isotopic compositions (Fig. 7). These lamproites show very low $^{176}Lu/^{177}Hf$ (0.0014–0.0043) and $^{147}Sm/^{144}Nd$ (0.076–0.096) ratios as in incompatible element-enriched mantle-derived rocks of such affinities. With the exception of two samples KLR-1 and KLP-1, which have initial ε_{Hf} values of +4.1 and −14.3, respectively, the other lamproites of our study display a narrow range of initial ε_{Hf} (−8.8 to −5.7) but variable initial ε_{Nd} values, all falling essentially on the crust–mantle array in Fig. 7. The initial ε_{Nd} values range from −11.5 to −6.0 for all those samples on the Nd–Hf array in Fig. 7. The majority of the Krishna lamproites (8 out of 10) define a similar horizontal array in the $\varepsilon_{Hf(T)}$–$\varepsilon_{Nd(T)}$ space (Fig. 7) parallel to global lamproites. Lamproites commonly display fairly restricted $\varepsilon_{Hf(T)}$ values for each suite at variable $\varepsilon_{Nd(T)}$ values. We believe this similarity reflects a common petrogenetic process in lamproite genesis.

Present day Pb-isotopic compositions of the lamproites are variable with extremely radiogenic composition (Table 3). The initial $^{206}Pb/^{204}Pb$ ratios of the lamproites range from 10.78–26.52, while those of the $^{207}Pb/^{204}Pb$ and $^{208}Pb/^{204}Pb$ ratios range from 15.11–

Table 3
Present day (0) and initial (T) Sr, Nd, Pb and Hf isotopic data of the Krishna lamproites and their corresponding Rb/Sr, Sm/Nd, Lu/Hf, U/Pb and Th/Pb ratios

Sample	$^{87}Rb/^{86}Sr$	$^{87}Sr/^{86}Sr(0)$	$^{87}Sr/^{86}Sr(T)$	$^{147}Sm/^{144}Nd$	$^{143}Nd/^{144}Nd(0)$	$\varepsilon_{Nd(0)}$	$\varepsilon_{Nd(T)}$	$^{176}Lu/^{177}Hf$	$^{176}Hf/^{177}$ Hf(0)	$\varepsilon_{Hf(0)}$	$\varepsilon_{Hf(T)}$
KLV-1	0.047	0.707198	0.706380	0.089	0.511282	−26.5	−9.6	0.0020	0.281790	−34.7	−8.4
KLV-2	0.014	0.705404	0.705162	0.088	0.511405	−24.1	−7.0	0.0015	0.281783	−35.0	−8.2
KLV-3	0.025	0.706999	0.706563	0.094	0.511422	−23.7	−7.7	0.0043	0.281922	−30.1	−5.7
KLJ-1	0.017	0.706947	0.706647	0.091	0.511396	−24.2	−7.7	0.0014	0.281781	−35.0	−8.2
KLJ-2	0.187	0.706981	0.703706	0.096	0.511354	−25.0	−9.3	0.0021	0.281834	−33.2	−6.9
Reddy	0.198	0.707466	0.703990	0.082	0.511372	−24.7	−6.7	0.0017	0.281770	−35.4	−8.8
Nalla	0.113	0.706188	0.704214	0.091	0.511481	−22.6	−6.0	0.0014	0.281805	−34.2	−7.4
KLP-1	1.994	0.735918	0.700961	0.076	0.511081	−30.4	−11.5	0.0015	0.281610	−41.1	−14.3
KLR-1	0.123	0.707802	0.705649	0.087	0.511373	−24.7	−7.5	0.0024	0.282151	−22.0	4.1
Th 3/1	0.124	0.706677	0.704501	0.097	0.511436	−23.4	−7.8	0.0023	0.281821	−33.6	−7.5

Sample	$^{238}U/^{204}Pb(\mu)$	$^{232}Th/^{204}Pb$	$^{206}Pb/^{204}Pb(0)$	$^{207}Pb/^{204}Pb(0)$	$^{208}Pb/^{204}Pb(0)$	$^{206}Pb/^{204}Pb(T)$	$^{207}Pb/^{204}Pb(T)$	$^{208}Pb/^{204}Pb(T)$
KLV-1	13.3	61.6	17.826	15.685	41.45	10.775	15.113	27.60
KLV-2	21.5	139.7	19.609	15.834	44.53	15.260	15.481	35.87
KLV-3	2.1	20.6	16.702	15.830	44.10	16.302	15.798	42.85
KLJ-1	28.6	165.8	20.187	16.038	45.51	14.281	15.559	35.02
KLJ-2	28.5	156.6	20.877	15.951	47.68	14.801	15.458	37.43
Reddy	8.2	58.4	17.040	15.465	39.21	15.553	15.344	35.95
Nalla	12.9	66.2	18.199	15.733	40.63	15.765	15.536	36.79
KLP-1	37.2	238.7	30.270	16.962	64.80	26.520	16.658	59.47
KLR-1	2.9	31.4	16.247	15.402	37.97	15.736	15.360	36.26
Th 3/1	17.0	129.1	20.024	15.871	49.10	16.372	15.575	40.60

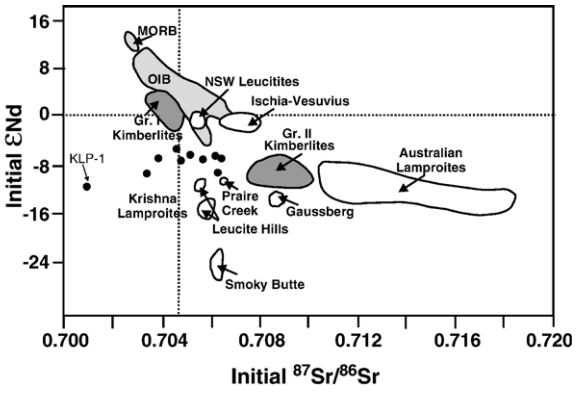

Fig. 6. Initial ε_{Nd} and $^{87}Sr/^{86}Sr$ for the Krishna lamproites (filled circles). Also shown are the Nd–Sr isotopic compositions of oceanic basalts, Group I and Group II kimberlites and other global lamproites (Mitchell and Bergman, 1991 and references therein). The Nd-isotopic composition of the Krishna lamproites overlap with those of the Group II kimberlites but their initial Sr-isotopic composition is comparatively unradiogenic. The anomalously unradiogenic Sr-isotopic composition of some samples like KLP-1 is perhaps due to over-correction of the initial ratios caused by post-emplacement mobilization of Rb and/or Sr (See Discussion).

16.66 and 27.60–59.47 respectively. The Pb-isotopic compositions of the lamproites are unusual as seen in the common Pb isotope space, where the initial $^{207}Pb/^{204}Pb$ ratios plot above and to the left of the 1.2 Ga-old

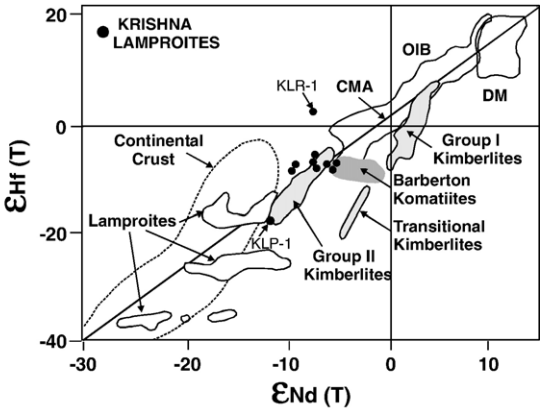

Fig. 7. Initial ε_{Nd}–ε_{Hf} for the Krishna lamproites (filled circles). Also shown are the fields of Group I, Group II and Transitional kimberlites, some global lamproites, Al-depleted Barberton komatiites calculated at 1224 Ma (Blichert-Toft and Arndt, 1999) oceanic basalts (OIB and DM) (Nowell et al., 2004) and Precambrian granites (continental crust) and the crust–mantle array (CMA) (Vervoort et al., 1999). The Krishna lamproites overlap with Group II kimberlites except for samples KLR-1 and KLP-1, which lie above and below the array respectively (see Discussion). The Hf-isotopic composition of the lamproites overlaps with those of the Al-depleted Barberton komatiites. Notice parallel trends in global lamproites as well as the Krishna lamproites of this study. See discussion for a possible cause of this parallel array off the crust–mantle array in the initial ε_{Nd}–ε_{Hf} correlation.

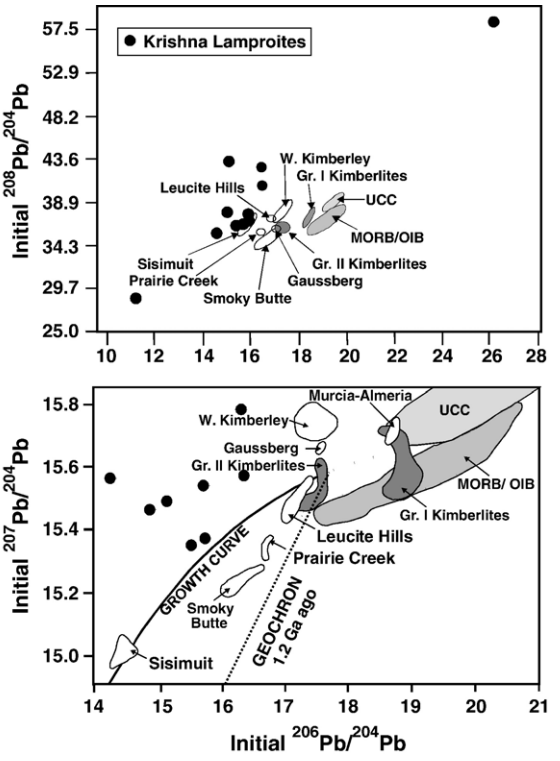

Fig. 8. Initial Pb-isotopic compositions for the Krishna lamproites are unusual with high $^{207}Pb/^{204}Pb$ and at low $^{206}Pb/^{204}Pb$ indicating presence of an Archean crustal component in the source. These rocks also have a variable but high $^{208}Pb/^{204}Pb$ at low $^{206}Pb/^{204}Pb$. Two lamproite samples, one with unusually high and the other with very low $^{208}Pb/^{204}Pb$ and $^{206}Pb/^{204}Pb$ values are shown in the upper diagram only. Also shown are the domains of MORB/OIB, Upper Continental Crust (UCC) (Zartman and Doe, 1981), Groups I and II kimberlites as well as other global lamproites (Mitchell and Bergman, 1991 and references therein).

geochron (Fig. 8). In general, these lamproites show characteristically high initial $^{207}Pb/^{204}Pb$ and $^{208}Pb/^{204}Pb$ values at correspondingly low initial $^{206}Pb/^{204}Pb$ values (Fig. 8).

5. Discussion

It is generally assumed that lamproites are generated by partial melting of a sub-continental lithospheric mantle source that was enriched by metasomatism prior to melting (Fraser et al., 1985; Mitchell and Bergman, 1991; Edgar and Mitchell, 1997; Rao et al., 2004). Other models involve subduction of Archean continent-derived sediments to the transition zone in the mantle (Murphy et al., 2002), as well as subducted recycled oceanic crust as a source component in the lamproites (Davies et al., 2006).

The extreme enrichment of the LREEs in lamproites, as high as 1000 times chondritic abundances, as seen in the Krishna lamproites documented above, precludes significant continental crustal contamination (Collerson and McCulloch, 1983; McCulloch et al., 1983; Fraser et al., 1985). This is also supported by the low SiO_2 contents (average 49%) of the Krishna lamproites and much higher concentration of the incompatible trace elements, such as Nb (average 147 ppm), Zr (average 930 ppm) and Sr (average 1225 ppm) compared with their continental crustal abundances. Lack of negative Nb anomaly (Fig. 3) coupled with the high concentration of Ni and Cr (Fig. 4) also indicates lack of a granitic crustal component in their magma source.

Krishna lamproites show nearly uniform but a very strong light-REE enriched pattern (Fig. 2) with variable but high U/Pb and Th/U ratios (Fig. 3). The extreme LREE enrichment is due to metasomatic enrichment of the mantle source prior to melting and also requires low degree partial melting with residual garnet in the magma source. The super-chondritic Zr/Hf (average 44.4) and Nb/Ta (average 23.6) of these lamproites also indicate metasomatic enrichment and partial melting with residual garnet. Absence of any Eu-anomaly in these rocks rules out the role of plagioclase either as a crystallizing or a residual phase in their petrogenesis. Some of the samples show negative Sr-anomalies (Fig. 3), which are possibly an artifact of post-emplacement weathering due to removal of some of the carbonate matrix of these rocks. High concentration of Ni indicates primitive nature of the magma and its linear relationship to MgO (Fig. 4) suggests contribution of olivine in the melt source. As the olivines in the lamproites occur as uniformly distributed phenocrysts without any evidence of crystal settling, the moderately high Mg-numbers (59–73) of these rocks indicate that they formed from a Mg-rich primitive source. Traditionally, high contents of LREEs and LILEs have either been explained by relatively large degree of partial melting of a metasomatised ultramafic mantle source or by very low degree melting of a normal garnet-bearing peridotitic mantle, enriched in K and other incompatible elements (Mitchell and Bergman, 1991). The above two scenarios were advanced to account for low-silica–high-magnesian lamproites and higher-silica–lower-magnesian lamproites, respectively. The low Al_2O_3/TiO_2 (1.1–4.2) and high CaO/Al_2O_3 ratios (average ~ 1.6) of these rocks are indicative of residual garnet in their source as also suggested for the sources of Al-depleted komatiites in the mantle (Blichert-Toft and Arndt, 1999; Campbell, 2002). The high Th/U ratio (average 6.9) can also be explained by the presence of garnet in the source of these rocks (LaTourrette et al., 1993) while the positive Zr anomalies in the primitive mantle-normalized plot (Fig. 3) are possibly due to the presence of perovskite in these rocks.

The Nd–Sr isotopic data of the Krishna lamproites show (Fig. 6) an overall negative correlation and most of them plot in the domain of negative ε_{Nd} and radiogenic Sr indicative of time-integrated high Rb/Sr and Nd/Sm ratios in their source. This correlation is also observed for other global lamproites (McCulloch et al., 1983). The anomalously unradiogenic initial Sr isotopic values for some of the samples plotting in the lower left section of Fig. 6 are possibly an artifact of surficial weathering of the lamproites that caused an increase in the Rb/Sr ratio of these rocks, resulting in over-correction of the initial Sr-isotopic ratios. For one sample (KLP-1) with very radiogenic present-day Sr-isotopic ratio (Table 3) and anomalously high Rb concentration (398 ppm), we postulate that post-emplacement Rb-enrichment due to surficial weathering in this monsoon-affected region must have increased the Rb/Sr ratio artificially, resulting in the extreme radiogenic Sr-isotopic composition ($^{87}Sr/^{86}Sr$= 0.73592) for this sample. For the remaining samples, loss of fluid-mobile Sr during post-emplacement removal of some of the carbonate matrix by the same surficial weathering could have resulted in over-correction of the initial Sr-isotopic values, but Rb-mobilization also cannot be ruled out for these samples. However, we believe that for most of the samples this over-correction is minimal and the Nd–Sr isotopic correlation as seen in Fig. 6 is representative of the source region.

The Sm–Nd and Lu–Hf isotope systematics of the Krishna lamproites (Fig. 7) show relatively coherent behavior and most of the data lie on the crust–mantle array (Vervoort et al., 1999; Bennett, 2004). Overall, the lamproites are isotopically similar to the global Group II kimberlites in this plot of Fig. 7 (Nowell et al., 2004). Present-day ε_{Nd} and ε_{Hf} values of the Krishna lamproites of this study (Table 3) are strongly negative trending towards the continental crustal domain (Vervoort et al., 1999) in Fig. 7. These negative values indicate the presence of an ancient and enriched component in their source with time-integrated low Lu/Hf and Sm/Nd ratios similar to those reported from Al-depleted komatiites (Blichert-Toft and Arndt, 1999). The initial Hf-isotopic compositions of most of the Krishna lamproites are also similar to those of Al-depleted Archean komatiites (Blichert-Toft and Arndt, 1999) when recalculated to 1224 Ma (age of the Krishna lamproites) (Fig. 7). These Archean Al-depleted komatiites of Fig. 7, however, show slightly more radiogenic Nd isotopic compositions compared to the Krishna

lamproites. We suggest that the variation in the initial Nd-isotopic composition of the Krishna lamproites at relatively constant initial Hf-isotopic ratios could result from varying degrees of carbonate metasomatism of the mantle source for the lamproites. These metasomatic fluids would characteristically have variable but low Sm/Nd and high Nd/Hf ratios with virtually no Hf due to its immobility in such fluids. These fluids created a veined and heterogeneous mantle source for the lamproites. It is our contention that the lamproite source acquired the variable and heterogeneous $\varepsilon_{Nd(T)}$ before partial melting resulting in the observed parallel array in the $\varepsilon_{Hf(T)}$–$\varepsilon_{Nd(T)}$ space similar to global lamproites (Fig. 7). We believe this similarity reflects a common petrogenetic process in lamproite genesis.

One of the samples of this study (KLR-1) shows a positive initial ε_{Hf} value (+4.1) although the corresponding initial ε_{Nd} value is strongly negative (−7.5) (Fig. 6). This discordant behavior may be interpreted as discussed above by low Sm/Nd and high Nd/Hf ratios of the metasomatic fluids in which Hf was relatively immobile relative to Nd (Ayers et al., 1997; Janey et al., 2005). However, the above scenario for the source-evolution of this sample in the mantle must have been different from the rest of the Krishna lamproites in that, perhaps a Group I kimberlite mantle source was involved in this case. Similarly, the least radiogenic lamproite sample of Fig. 7 (KLP-1) must have experienced a different evolutionary history in the mantle, unlike the other lamproites but similar to Group II kimberlites.

The lamproites have an average Nb/U ratio of 59 and an average Nb/Th ratio of 9 that overlap with those of Archean komatiites (Fig. 5) (Sylvester et al., 1997; Puchtel et al., 1998; Xie et al., 2000; Polat and Kerrich, 2000; Campbell, 2002). The very high Nb/U in some of the lamproite samples is possibly due to secondary U-loss from weathering. The Nb/Th ratios of the lamproites are however, similar to the Archean komatiites.

The Krishna lamproites have a wide range in their Pb-isotopic composition (Table 3) and have characteristically high initial $^{207}Pb/^{204}Pb$ (15.11–16.66) and $^{208}Pb/^{204}Pb$ (27.6–59.5) ratios at correspondingly low initial $^{206}Pb/^{204}Pb$ values (10.78–26.52) (Fig. 8) requiring their source evolution in a high U/Pb, high Th/Pb environment early in earth history. In a combined $^{207}Pb/^{204}Pb$ vs. $^{206}Pb/^{204}Pb$ plot, these rocks plot to the left of the 1.2 Ga geochron unlike most mantle-derived rocks. This Pb-isotopic signature along with superchondritic Nb/Ta ratios (average 23.6) cannot be explained by derivation from a metasomatized subcontinental lithospheric mantle, which is characterized by low Nb/Ta ratios (Murphy et al., 2002).

The high initial $^{207}Pb/^{204}Pb$ at low initial $^{206}Pb/^{204}Pb$ values (Fig. 8), also observed in other lamproites such as in the 56 ka-old Gaussberg lamproites (Murphy et al., 2002), indicate presence of an Archean crustal component in the source. Archean komatiites also have very low initial $^{206}Pb/^{204}Pb$ ratios at comparatively high $^{207}Pb/^{204}Pb$ values (Dupre and Arndt, 1990; Carignan et al., 1995). In addition, komatiitic flows are often associated with sulfide deposits. Segregation of Pb in sulfides during metasomatism/metamorphism of a subducted komatiite or during subduction could result in high time integrated U/Pb and Th/Pb ratios, required to generate the observed highly radiogenic Pb isotopic composition of the lamproites. Low concentration of the platinum group elements (PGE) in the Krishna lamproites (Paul et al., in preparation) as well as the negative Pb anomaly observed in the primitive mantle-normalized plots (Fig. 3) may indicate that the sulfide-sequestered PGE and Pb remained segregated in the subducted komatiites and did not participate in generation of the lamproite melt.

Komatiites are ultramafic lavas that are characterized by high MgO content (>18%), high NiO and Cr_2O_3, moderate to low SiO_2 (~45%) and were generated more commonly in the Archean and Proterozoic. Al-depleted komatiites are comparatively less siliceous and more magnesian and Ni-rich compared to the Al-undepleted komatiites (Polat et al., 1999). Al-depleted komatiites also have an HREE-depleted pattern compared to Al-undepleted komatiites, which show a flat HREE pattern (Nesbitt et al., 1979; Blichert-Toft and Arndt, 1999). In addition, Al-depleted komatiites have high Th/U (4–5), CaO/Al_2O_3 >1, as well as subchondritic Al_2O_3/TiO_2, indicative of residual garnet in their source (Sun and Nesbitt, 1978; Campbell, 2002). The Krishna lamproites are also characterized by high Th/U (average 6.9), low Al_2O_3/TiO_2 ratios (1.1–4.2) and an average CaO/Al_2O_3 of ~1.6, very similar to Al-depleted komatiites. Alternatively, this could also indicate the presence of residual garnet in the source of the Krishna lamproites.

We are proposing here a model for lamproite petrogenesis, on the basis of the geochemical characteristics of Krishna lamproites and other general observations on global lamproites, with the primary requirement that a subducted Archean or an ancient Al-depleted komatiitic component was present in the source of the lamproites along with the ambient peridotitic mantle. This model is constrained by the lamproite's geochemical signatures, specifically, their Nd–Hf–Pb isotopic characteristics, low SiO_2, high Mg-numbers, low Al_2O_3/TiO_2, high CaO/Al_2O_3, high TiO_2, high Ni, Cr, Th/U and Nb/Th–Nb/U ratios. In this model we

specifically recognize the need for a metasomatized source in the mantle and suggest that the source was not basaltic or granitic but more basic than these two rock types with lower silica contents than a basalt — as in a metasomatized komatiite–peridotite source, so that the partial melting product, which is the Krishna lamproite in this case, is also generally low in silica but high in K and other incompatible elements. This crust–mantle assemblage was variably metasomatized with LILE, especially K, and LREE, although the agent of metasomatism remains unclear. However, this agent most likely was CO_2, H_2O-enriched with subducted Nd, Pb, and Sr in variable amounts. This scenario of partial melting of the komatiitic crust in the presence of olivine-rich peridotitic mantle may explain the major element compositions, such as K, Mg, Si, Al as well as Ni and Cr of the lamproites in addition to the lithophile isotopic tracers of Nd, Pb, Hf and Sr and their parent isotopes.

Our proposed komatiite melting model for the genesis of the Krishna lamproites might also be applicable for other global lamproites from cratonic settings, since older komatiite-bearing subducted crust were possibly ubiquitous components of the ancient cratonic mantle.

6. Conclusions

Our trace element and combined Nd–Sr–Hf–Pb isotopic study of the Krishna lamproites, one of the oldest such rocks (ca 1.2 Ga) in the world, provides an insight into deep subcontinental mantle processes actively operating at that time in the southern Indian craton. Based on our geochemical and isotopic data, we propose a model in which lamproites are generated by partial melting of a subducted Al-depleted komatiite bearing mantle peridotite source assemblage, which was metasomatized prior to melting. Partial melting of such a source would generate LREE enriched melts with komatiite-like Nb/U and Nb/Th, low Al_2O_3/TiO_2, high CaO/Al_2O_3, high Ni, Cr, along with low SiO_2contents and high Mg-numbers as seen in the Krishna lamproites. Presence of a subducted Al-depleted and metasomatically enriched komatiitic component can also account for the time-integrated low Sm/Nd and low Lu/Hf ratios in the source required to explain the Nd–Hf isotopic characteristics of the lamproites. The high initial $^{207}Pb/^{204}Pb$ and $^{208}Pb/^{204}Pb$ at low initial $^{206}Pb/^{204}Pb$ ratios of the lamproites are similar to Archean komatiites and indicate their evolution in high U/Pb and Th/Pb environments early in the earth's history. High U/Pb in the melt source could be due to segregation of sulfides associated with subducted komatiites in the mantle. Our proposed komatiite melting model for the genesis of the Krishna lamproites might also be applicable for other global lamproites from cratonic settings, since older komatiite-bearing subducted crust were possibly ubiquitous components of the ancient cratonic mantle.

Acknowledgements

This research was partially supported by NSF grants to ARB. DKP thanks CSIR, Government of India, for financial support. We thank Drs. Y. Liu and J. D. Barling for providing technical assistance in trace element and Hf-isotopic analysis, respectively, in the ICPMS laboratory. This paper benefited from critical and helpful reviews and suggestions by Drs. A. Polat and S. L. Goldstein and an anonymous reviewer.

References

Ayers, J.C., Dittmer, S.K., Layne, G.D., 1997. Partitioning of elements between peridotite and H_2O at 2.0–3.0 GPa and 900–1100 C, and application to models of subduction zone processes. Earth and Planetary Science Letters 150, 381–398.

Basu, A.R., Tatsumoto, M., 1979. Sm–Nd systematics in kimberlites and in the minerals of garnet lherzolite inclusions. Science 205, 398–401.

Basu, A.R., Sharma, M., DeCelles, P.G., 1990. Nd, Sr-isotopic provenance and trace element geochemistry of Amazonian Foreland Basin Fluvial Sands, Bolivia and Peru: implications for Ensialic Andean Orogeny. Earth and Planetary Science Letters 105, 149–169.

Bennett, V.C., 2004. Compositional Evolution of the mantle, Treatise on Geochemistry. Elsevier/Pergamon, Amsterdam/Boston, pp. 493–519.

Bizzarro, M., Baker, J.A., Haack, H., Ulfbeck, D., Rosing, M., 2003. Early history of Earth's crust–mantle system inferred from hafnium isotopes in chondrites. Nature 421 (6926), 931–932.

Blichert-Toft, J., Albarede, F., 1997. The Lu–Hf isotope geochemistry of chondrites and the evolution of the mantle–crust system. Earth and Planetary Science Letters 148, 243–258.

Blichert-Toft, J., Arndt, N.T., 1999. Hf isotopic composition of komatiites. Earth and Planetary Science Letters 171, 439–451.

Blichert-Toft, J., Chauvel, C., Albarede, F., 1997. Separation of Hf and Lu for high-precision isotope analysis of rock samples by magnetic sector-multiple collector ICP-MS. Contributions to Mineralogy and Petrology 127, 248–260.

Campbell, I.H., 2002. Implications of Nb/U, Th/U and Sm/Nd in plume magmas for the relationship between continental and oceanic crust formation and the development of the depleted mantle. Geochimica et Cosmochimica Acta 66 (9), 1651–1661.

Carignan, J., Machado, N., Gariepy, C., 1995. U–Pb isotope geochemistry of komatiites and pyroxenes from the southern Abitibi greenstone belt, Canada. Chemical Geology 126, 17–27.

Collerson, K.D., McCulloch, M.T., 1983. Nd and Sr isotope geochemistry of leucite-bearing lavas from Gaussberg, East Antarctica. In: Oliver, R.L., James, P.R., Jago, J.B. (Eds.), Antarctic Earth Science; Fourth International Symposium. Cambridge University Press, pp. 676–680.

Cullers, R.L., Ramakrishnan, S., Berendsen, P., Griffin, T., 1985. Geochemistry and petrogenesis of lamproites, late Cretaceous age, Woodson County, Kansas, U.S.A. Geochimica et Cosmochimica Acta 49, 1388–1402.

Davies, G.R., Stolz, A.J., Mahotkin, I.L., Nowell, G.M., Pearson, D.G., 2006. Trace element and Sr–Pb–Nd–Hf isotope evidence for ancient, fluid-dominated enrichment of the source of Aldan Shield lamproites. Journal of Petrology 47 (6), 1119–1146.

Dupre, B., Arndt, N.T., 1990. Pb isotopic compositions of Archean komatiites and sulfides. Chemical Geology 85, 35–56.

Edgar, A.D., Mitchell, R.H., 1997. Ultra-high pressure–temperature melting experiments on a SiO_2 rich lamproite from Smoky Butte, Montana: derivation of siliceous lamproite magmas from enriched sources deep in the continental mantle. Journal of Petrology 38, 457–477.

Foley, S.F., Venturelli, G., Green, D.H., Toscani, L., 1987. The ultrapottasic rocks: characteristics, classification and constraints for petrogenetic models. Earth-Science Reviews 24, 81–134.

Fraser, K.J., Hawkesworth, C.J., Erlank, A.J., Mitchell, R.H., Scott-Smith, B.H., 1985. Sr, Nd and Pb isotope and minor element geochemistry of lamproites and kimberlites. Earth and Planetary Science Letters 76, 57–70.

Jacobsen, S.B., Wasserburg, G.J., 1980. Sm–Nd evolution of chondrites. Earth and Planetary Science Letters 50, 139.

Janey, P.E., Le Roex, A.P., Carlson, R.W., 2005. Hafnium isotopic and trace element constraints on the nature of mantle heterogeneity beneath the central southwest Indian ridge. Journal of Petrology 46, 2427–2464.

Kramers, J.D., Smith, C.B., Lock, N.P., Harmon, R.S., Boyd, F.R., 1981. Can kimberlites be generated from an ordinary mantle. Nature 291, 53–56.

Kumar, A., Gopalan, K., Rao, K.R.P., Nayak, S.S., 2001. Rb–Sr age of kimberlites and lamproites from Eastern Dharwar craton, South India. Journal Geological Society of India 58, 135–141.

LaTourrette, T.Z., Kennedy, A.K., Wasserburg, G.J., 1993. Thorium–uranium fractionation by garnet: evidence for a deep source and rapid rise of oceanic basalts. Science 261.

McCulloch, M.T., Jaques, A.L., Nelson, D.R., Lewis, J.D., 1983. Nd and Sr isotopes in kimberlites and lamproites from Western Australia: an enriched mantle origin. Nature 302, 400–403.

Mitchell, R.H., Bergman, S.C., 1991. Petrology of Lamproites. Plenum Press, New York. 447 pp.

Murphy, D.T., Collerson, K.D., Kamber, B.S., 2002. Lamproites from Gaussberg, Antarctica: possible transition zone melts of Archean subducted sediments. Journal of Petrology 43 (6), 981–1001.

Nesbitt, R.W., Sun, S.-S., Purvis, A.C., 1979. Komatiites: geochemistry and genesis. Canadian Mineralogist 17, 165–186.

Nowell, G.M., et al., 2004. Hf isotope systematics of Kimberlites and their megacrysts: new constraints on their source regions. Journal of Petrology 45 (8), 1583–1612.

O'Nions, R.K., Hamilton, P.J., Evensen, N.M., 1977. Variations in 143Nd/144Nd and 87Sr/86Sr ratios in oceanic basalts. Earth and Planetary Science Letters 34, 13–22.

Paul, D.K., Crocket, J.H., Reddy, T.A.K., Pant, N.C., in preparation. Petrology and Geochemistry including Platinum element abundances of the Mesoproterozoic ultramafic (Lamproite) rocks of Krishna district, Southern India: Implications for source characteristics and petrogenesis.

Polat, A., Kerrich, R., 2000. Archean greenstone belt magmatism and the continental growth-mantle evolution connection: constraints from Th–U–Nb–LREE systematics of the 2.7 Ga Wawa subprovince, Superior Province, Canada. Earth and Planetary Science Letters 175, 41–54.

Polat, A., Kerrich, R., Wyman, D.A., 1999. Geochemical diversity in oceanic komatiites and basalts from the late Archean Wawa greenstone belts, Superior Province, Canada: trace element and Nd isotope evidence for a heterogeneous mantle. Precambrian Research 94, 139–173.

Puchtel, I.S., et al., 1998. Oceanic plateau model for continental crustal growth in the Archean: a case study from the Kostomuksha greenstone belt, NW Baltic Shield. Earth and Planetary Science Letters 155, 57–74.

Rao, N.V.C., Gibson, S.A., Pyle, D.M., Dickin, A.P., 2004. Petrogenesis of Proterozoic lamproites and kimberlites from the Cuddapah Basin and Dharwar Craton, Southern India. Journal of Petrology 45, 907–948.

Sharma, M., Basu, A.R., Nesterenko, G.V., 1992. Temporal Sr, Nd and Pb isotopic variations in the Siberian flood basalts: implications for the plume-source characteristics. Earth and Planetary Science Letters 113, 365–381.

Skinner, E.M.W., Smith, C.B., Bristow, J.W., Scott-Smith, B.H., Dawson, J.B., 1985. Proterozoic kimberlites and lamproites and a preliminary age for the Argyle pipe, Western Australia. Transactions of the Geological Society of South Africa 88, 335–340.

Sun, S.-S., McDonough, W.F., 1989. Chemical and isotopic systematics of oceanic basalts: implications for mantle composition and processes. Magmatism in the ocean basins. Geological Society Special Publication 42.

Sun, S.-S., Nesbitt, R.W., 1978. Petrogenesis of Archean ultrabasic and basic volcanics: evidence from rare earth elements. Contributions to Mineralogy and Petrology 65, 301–325.

Sylvester, P.J., Campbell, I.H., Bowyer, D.A., 1997. Niobium/uranium evidence for early formation of the continental crust. Science 275, 521–523.

Vervoort, J.D., Patchett, P.J., Blichert-Toft, J., Albarede, F., 1999. Relationships between Lu–Hf and Sm–Nd isotopic systems in the global sedimentary system. Earth and Planetary Science Letters 168, 79–99.

Woolley, A.R., et al., 1996. Classification of lamprophyres, lamproites, kimberlites, and the kalsilitic, melilitic, and leucitic rocks. The Canadian Mineralogist 34, 175–186.

Xie, Q., Kerrich, R., Fryer, B., 2000. U–Th–Nb–La systematics of Archean komatiites from the 2.7 Ga Abitibi Sub-province: implications for the formation of continental crust and lithosphere recycling. Journal of Conference Abstracts 5 (2), 1107.

Zartman, R.E., Doe, B.R., 1981. Plumbotectonics — the model. Tectonophysics 75, 135–162.